Neurobiology of Disease 124 (2019) 544–554

Contents lists available at ScienceDirect

Neurobiology of Disease

journal homepage: www.elsevier.com/locate/ynbdi

Low cerebral blood flow is a non-invasive biomarker of neuroinflammation after repetitive mild traumatic brain injury

Sitara B. Sankar[a,b,1], Alyssa F. Pybus[a,b,1], Amanda Liew[a], Bharat Sanders[a], Kajol J. Shah[a], Levi B. Wood[a,b,c,*,2], Erin M. Buckley[a,d,*,2]

[a] Wallace H. Coulter Department of Biomedical Engineering, Georgia Institute of Technology and Emory University, USA
[b] Parker H. Petit Institute for Bioengineering and Bioscience, Georgia Institute of Technology, USA
[c] George W. Woodruff School of Mechanical Engineering, Georgia Institute of Technology, USA
[d] Department of Pediatrics, School of Medicine, Emory University, USA

ARTICLE INFO

Keywords:
Cerebral blood flow
Cytokines
Mild traumatic brain injury
Neuroinflammation
Kinase signaling

ABSTRACT

Previous work has shown that non-invasive optical measurement of low cerebral blood flow (CBF) is an acute biomarker of poor long-term cognitive outcome after repetitive mild traumatic brain injury (rmTBI). Herein, we explore the relationship between acute cerebral blood flow and underlying neuroinflammation. Specifically, because neuroinflammation is a driver of secondary injury after TBI, we hypothesized that both glial activation and inflammatory signaling are associated with acute CBF and, by extension, with long-term cognitive outcome after rmTBI. To test this hypothesis, cortical CBF was non-invasively measured in anesthetized mice 4 h after 3 repetitive closed head injuries spaced once-daily, at which time brains were collected. Right hemispheres were fixed for immunohistochemical staining for glial activation markers Iba1 and GFAP while left hemispheres were used to quantify Iba1 and GFAP expression via Western blot as well as 32 cytokines and 21 phospho-proteins in the MAPK, PI3K/Akt, and NF-κB pathways using a Luminex multiplexed immunoassay. N = 8/7 injured/sham C57/black-6 adult male mice were studied. Within the injured group, CBF inversely correlated with Iba1 expression ($R = -0.86$, $p < .01$). Further, partial least squares regression analysis revealed significant correlations between CBF and expression of multiple pro-inflammatory cytokines, including RANTES and IL-17. Finally, within the injured group, phosphorylation of specific signals in the MAPK and NF-κB intracellular signaling pathways (e.g., p38 MAPK and NF-κB) were significantly positively correlated with Iba1. In total, our data indicate that acute cerebral blood flow after rmTBI is a biomarker of underlying neuroinflammatory pathology.

1. Introduction

Repetitive head impacts sustained within a window of vulnerability can lead to cumulative severity of injury that can last longer than the effects of a single head impact alone (Guskiewicz et al., 2003) and lead to permanent neurodegeneration (Barkhoudarian et al., 2016; IOM and NRC, 2014; Longhi et al., 2005). The consequences of repetitive head impacts are especially relevant in football and other high impact contact sports, where players can be exposed to hundreds of sub-concussive head impacts each season (Forbes et al., 2012), and where cognitive impairments have been detected even in the absence of diagnosed concussion (Talavage et al., 2014). Moreover, a recent study of retired American football players demonstrated that ~90% had evidence of chronic traumatic encephalopathy, along with numerous molecular hallmarks of Alzheimer's disease, including amyloid beta plaques and neurofibrillary tangles (Mez et al., 2017).

Given the high incidence and serious consequences of sports-related mild traumatic brain injury (mTBI), non-invasive biomarkers that can be used to diagnose injury severity post-impact and/or to identify patients who could benefit most from early rehabilitation could become an important component of individualized patient care (da Costa et al., 2016; Meehan et al., 2012; Meier et al., 2015). Several clinical and preclinical studies have demonstrated that reduced cerebral blood flow after TBI may be one such biomarker (da Costa et al., 2016; Liu et al.,

Abbreviations: CBF, Cerebral Blood Flow; CHI, Closed-Head Injury; rmTBI, Repetitive Mild Traumatic Brain Injury; PLSR, Partial Least Squares Regression; LV, Latent Variable; LOOCV, Leave One Out Cross Validation; DCS, Diffuse Correlation Spectroscopy; NO, Nitric Oxide

* Corresponding authors.
E-mail addresses: levi.wood@me.gatech.edu (L.B. Wood), erin.buckley@emory.edu (E.M. Buckley).
[1] Equally contributing first and second authors.
[2] Equally contributing corresponding authors.

https://doi.org/10.1016/j.nbd.2018.12.018
Received 13 September 2018; Received in revised form 4 December 2018; Accepted 24 December 2018
Available online 25 December 2018
0969-9961/

2013; Meier et al., 2015). Indeed, data from our own group has shown that cerebral blood flow (CBF) can be an acute biomarker of longer term cognitive outcome in a mouse model of repetitive mTBI that is biomechanically akin to a mild sub-concussive injury in humans (Buckley et al., 2015; Meehan et al., 2012; Wu et al., 2018). Specifically, using a five hit once-daily repetitive closed head injury model (5xCHI), mice with low CBF after the third CHI were more likely to suffer worse long-term deficits in spatial learning and memory after 5xCHI (Buckley et al., 2015).

Having previously found that low acute CBF is associated with worse long-term cognitive outcomes after rmTBI, we aimed to characterize underlying acute molecular and pathophysiologic changes that correlate with acute CBF post-injury and, by extension, that potentially drive worse long-term outcomes after repetitive mTBI. One mechanism that may drive long-term outcome after rmTBI is neuroinflammation. The neuroinflammatory response post-mTBI includes astrocyte and microglial activation and over-expression of cytokines and chemokines (Giza and Hovda, 2014). Numerous elements of neuroinflammation have been shown to directly or indirectly regulate vascular tone. For example, activated glia can produce nitric oxide (NO), a potent vasodilator (Chao et al., 1992), as well as vasomodulatory prostaglandins (Armstead, 2006; Ikeda-Matsuo et al., 2005). Additionally, cytokines such as IL-2 and IFN-γ stimulate microglial production of NO (Goodwin et al., 1995; Hanisch et al., 1996), while others, such as IL-15, can suppress NO production (Hanisch et al., 1997). Thus, there is strong evidence to suggest that neuroinflammatory factors may drive changes in CBF after repetitive mTBI. By understanding which neuroinflammatory processes are associated with changes in acute CBF after repetitive mTBI, we can begin to uncover the mechanisms that link acute neuroinflammation, cerebral blood flow, and longer-term cognitive outcome.

In the present study, we used an established mouse model of repetitive mTBI to test the hypothesis that low CBF in the acute phase after injury is a biomarker of both increased glial activity as well as pro-inflammatory cytokine expression. Further, because glial activation and cytokine expression are regulated by intracellular signaling, we hypothesized that pro-inflammatory signaling pathways would be acutely elevated in injured mice and that the extent to which they are elevated would positively correlate with markers of neuroinflammation, i.e., GFAP and/or Iba1. Because we have previously showed that CBF 4 h after 3 repetitive closed head injuries spaced once-daily (3xCHI) is strongly correlated with subsequent cognitive outcome after animals undergo a total of 5 once-daily repetitive insults (Buckley et al., 2015), herein we employed the same injury model while focusing specifically on the acute time point of 4 h after 3xCHI. The present study is part of a larger ongoing body of work that aims to characterize the temporal evolution of both hemodynamic and neuroinflammatory changes that accompany this repetitive mild TBI model, as well as the complex interplay between blood flow and neuroinflammation post-rmTBI.

2. Materials and methods

2.1. Study protocol

Adult male C57BL/6 mice from Jackson Laboratory were used. All protocols were approved by the Emory University Institutional Animal Care and Use Committee in accordance with National Institutes of Health guidelines, and study design and data analysis follow all appropriate ARRIVE guidelines. Mice were housed in a pathogen free facility with a twelve-hour light/dark cycle. Food and water were provided ad libitum. Mice were randomly assigned to one of two groups: three closed head injuries spaced once daily (3xCHI) or sham-injured controls. Cerebral blood flow was measured at baseline and 4 h after the final closed head injury, at which time the animal was sacrificed and the brain was harvested for molecular and pathological assessment. In total, nine 3xCHI and seven sham-injured mice were studied. Mice were four months old with a mean (SEM) weight of 28.7 (0.5) g. One 3xCHI injured mouse was sacrificed prior to the study end point due to prolonged apnea after impact. All other mice were included in the data analysis, and group identities were known.

2.2. Closed head injury model

This work was conducted using a previously characterized weight drop closed head injury model (Meehan et al., 2012). To induce injury, mice were anesthetized with 4.5% isoflurane (1 L/min, 70/30 nitric oxide/oxygen) for forty-five seconds. Animals were then placed prone on a Kimwipes® task wipe (Kimberly-Clark, Irving, TX), grasped by the base of the tail, and the dorsal aspect of the skull was positioned directly under a vertically-mounted 96.5 cm guide tube (49035K85, McMaster-Carr, Elmhurst IL). A 54 g bolt was released from the top of the tube to deliver a closed-head impact (CHI) between the coronal and lambdoid sutures of the intact skull/scalp. At impact, the mouse and bolt penetrated the task wipe, allowing for rapid unrestricted rotation of the head in the anterior-posterior plane. Control, sham-injured mice were age- and sex- matched and received the same exposure to anesthesia but were not subject to closed-head injury.

2.3. Measurements of cerebral blood flow

Cerebral blood flow (CBF) measurements were performed using Diffuse Correlation Spectroscopy (DCS), as previously described (Buckley et al., 2015). Briefly, DCS measures temporal fluctuations in reflected near-infrared light intensity on the tissue surface, which are primarily caused by moving red blood cells. Analytical models are used to relate these intensity fluctuations to a quantitative index of CBF (i.e., CBF_i). The units of this index [mm^2/s] are not the traditional units of cerebral blood flow [mL/min/100 g]; however, numerous validation studies with other “gold standard” blood flow modalities have demonstrated that this index correlates strongly with volumetric blood flow (recently reviewed in Durduran and Yodh, 2014). Herein, for simplicity we report CBF_i in [a.u.], where 1 a.u. is equivalent to 1e-5 mm^2/s. We use a custom-built DCS instrument consisting of an 852 nm long-coherence length laser (CrystaLaser, Reno LV), a photon counting avalanche photodiode (Perkin-Elmer), and a hardware autocorrelator board (www.correlator.com). The animal interface consists of a custom optical sensor configured with a single source (Fiberoptics Technology, Inc., Pomfret, CT) and detector (780HP, Thorlabs, Newton, NJ) fiber spaced 6 mm apart and embedded in a rigid black 3D printed housing. With this source-detector geometry, the measured blood flow index represents a mean value of the microvascular CBF within a banana-shaped region spanning from source to detector that reaches an average depth from the surface of the scalp of roughly 2–3 mm (Patterson et al., 1995).

DCS measurements of cerebral blood flow were obtained in anesthetized animals 5 min prior to the first CHI/sham-CHI to determine a baseline CBF value, as well as 4 h after the third injury/sham-injury. Depilatory cream was used to remove hair from the scalp three days prior to the baseline measurements in order to improve signal-to-noise ratio. For each CBF measurement session, mice were induced at 4.5% isoflurane (1 L/min, 70/30 nitric oxide/oxygen) for forty-five seconds and then maintained at 1.5% isoflurane via nose cone. After 1 to 2 min of stabilization, the optical sensor was gently placed over the intact scalp such that the source and detector fibers aligned with the parasagittal plane (source fiber approximately at bregma −1, 3 mm mediolateral). DCS data was acquired for 5 s over each hemisphere; measurements were repeated 3 × /hemisphere and averaged to yield a mean CBF_i for the right and left hemisphere. Data was discarded according to pre-defined objective quality metrics (Buckley et al., 2015).

2.4. Western blot

Western blot was used for quantification of Iba1 and GFAP in the brain 4 h after the final closed head injury. Cortical and hippocampal brain tissues from the left brain hemisphere of each animal were lysed using the Bio-Plex cell lysis kit (Bio-Rad, Hercules, CA), with the addition of cOmplete™ mini protease inhibitor tablet (Roche, Basel, Switzerland) and 2 mM phenylmethylsulfonyl fluoride (Sigma). Lysates were stored at −80 °C until analysis. Protein concentrations were determined using a Pierce BCA Protein Assay (Thermo Fisher). Prior to analysis, lysates were thawed on ice and centrifuged at 4 °C for 10 min at 13 kRPM. Twenty μg of protein was dissolved in reducing sample buffer, boiled, and loaded onto 4–15% Mini-PROTEAN® TGX™ Precast Protein Gels (Bio-Rad). Following separation by electrophoresis, proteins were transferred to a Hybond P 0.45 μm polyvinylidene fluoride membrane (GE Healthcare, Piscataway, NJ). Membranes were blocked at room temperature for 1 h with Odyssey Blocking Buffer (OBB) (LI-COR Biosciences, Lincoln, NE) and then probed at 4 °C overnight with anti-Iba1 (1:1000, Invitrogen), anti-GFAP (1:5000, Novus Biologicals), and anti-GAPDH (1:5000, Sigma). Membranes were rinsed then incubated with Alexa Fluor 680 or 790 secondary antibodies (1:2000, Invitrogen) for 1 h at room temperature. Imaging of blots was performed using an Odyssey CLx Imager (LI-COR Biosciences). Protein quantification was performed using Image Studio Lite 5.2 (LI-COR Biosciences) and Iba1/GFAP values were normalized to GAPDH. For cortical 3xCHI samples, Iba1 values reported were averaged over two technical replicates on separate blots, and the values on each blot were normalized via a linear regression. Cortical sham controls were run on a separate blot and Iba1 values were normalized to a replicate run on both the sham membrane and one of the 3xCHI membranes.

2.5. Quantification of cytokines and phospho-proteins

An array of cytokines and phospho-proteins within signaling pathways that regulate transcription of inflammatory factors, i.e., mitogen activated protein kinase (MAPK), phosphoinositide 3-kinase/Akt (PI3K/Akt), and nuclear factor kappa-light-chain-enhancer of activated B cells (NF-κB), were quantified from brain tissue harvested 4 h after the final closed head injury. Cortical and hippocampal tissue lysates were obtained and concentrations determined as described in the Western Blot section. Prior to analysis, lysates were thawed on ice and centrifuged at 4 °C for 10 min at 13 kRPM. Protein concentrations were normalized with Milliplex® MAP Assay Buffer (EMD Millipore, Billerica, MA) to 12 μg protein per 12.5 μL for cytokines, 2 μg protein per 12.5 μL for the Akt/mTor pathway, 10 μg protein per 12.5 μL for the MAPK pathway, and 1.5 μg per 6.25 μL for the NF-κB pathway. These protein concentrations were selected because they fell within the linear range of bead fluorescent intensity vs. protein concentration for detectable analytes. Multiplexed cytokine quantification was conducted using the Milliplex® MAP Mouse Cytokine/Chemokine 32-Plex Kit (Eotaxin, G-CSF, GM-CSF, IFN-γ, IL-1α, IL-1β, IL-2, IL-3, IL-4, IL-5, IL-6, IL-7, IL-9, IL-10, IL-12p40, IL-12p70, IL-13, IL-15, IL-17, IP-10, KC, LIF, LIX, MCP-1, M-CSF, MIG, MIP-1α, MIP-1β, MIP-2, RANTES, TNF-α, and VEGF) (EMD Millipore). Multiplexed phospho-protein quantification was conducted for the Akt/mTOR, MAPK, and NF-κB signaling pathways using the Milliplex® MAP Akt/mTOR 11-Plex (p-Akt, p-GSK3α/β, p-IGF1R*,p-IR, p-IRS1, p-mTOR, p-p70S6K*, p-PTEN*, p-RPS6*, and p-TSC2), MAPK/SAPK 10-Plex (p-ATF2, p-Erk, p-HSP27*, p-JNK, p-c-Jun, p-MEK1, p-MSK1, p-p38, p-p53), and NF-κB 6-Plex (c-Myc*, p-FADD, p-IκBα, p-IKKα/β, p-NF-κB, TNFR1) phospho-signaling magnetic bead kits (EMD Millipore). Cytokine and phospho-protein signaling kits were read on a MAGPIX® system (Luminex, Austin, TX). Phospho-proteins marked with an asterisk did not fall within a linear range and were not included in our analysis.

2.6. Immunohistochemistry

Immunohistochemistry was used to investigate Iba1, NeuN, RANTES, phospho-p38, and phospho-NF-κB. Right brain hemispheres from each animal were fixed in 4% paraformaldehyde, paraffin processed, and embedded. Tissue slices were cut into 7 μm thick sagittal sections using a rotary microtome (Thermo Fisher) and affixed onto glass microscope slides (Electron Microscopy Sciences, Hatfield, PA). Tissue slices were deparafinized in xylenes and rehydrated by washing with 100% ethanol, 95% ethanol, and deionized water. Antigen retrieval was performed in a microwave by boiling slides in 10 mM sodium citrate buffer at pH 6.0. Slides were rinsed in tris-buffered saline with 0.01% tween (TBST). A hydrophobic ring was drawn around each individual tissue slice using an immunohistochemistry PAP pen (Enzo Life Sciences, Farmingdale, NY), after which samples were blocked for 1 h in OBB. Samples were incubated at 4 °C overnight with primary antibodies diluted in OBB: anti-Iba1 (1:100, Invitrogen), anti-p38 (Thr180, Tyr182) (1:200, Cell Signaling Technology, Danvers, MA), anti-NF-κB p65 (phospho S536) (1:500, Abcam, Cambridge, MA), anti-RANTES (1:50, Invitrogen) and anti-NeuN (1:200, Abcam), as appropriate. Slides were rinsed again in TBST and incubated with either Alexa Fluor 555 or Alexa Fluor 647 secondary antibodies, diluted 1:200 in OBB. Slides were counterstained with 1 μg/uL DAPI, rinsed, and mounted with VECTASHIELD Antifade Mounting Medium (Vector Laboratories, Burlingame, CA). Samples were imaged using epi-fluorescent or confocal microscopy, on a Zeiss Axio Observer Z.1 inverted microscope or a Zeiss LSM 700 laser scanning inverted microscope, respectively.

2.7. Statistical analysis and partial least squares regression

Data are presented as mean ± standard error of the mean (SEM) unless otherwise stated. Unpaired, two-sided *t*-tests were used to test for differences in CBF_i and Iba1 between sham and injured groups. To quantify the relationship between CBF_i and either Iba1 or selected cytokines, or between Iba1 and selected phospho-proteins, we fit least squares linear regression models and reported Pearson's correlation coefficient, R, together with the p-value calculated from an F test using the null hypothesis that the overall slope is zero. For all analysis, $p < .05$ was considered statistically significant. All analyses were performed using GraphPad Prism 7 (GraphPad Software, La Jolla, CA).

Multivariate cytokine and phospho-protein signaling data were analyzed using partial least squares regression (PLSR) or discriminant partial least squares regression (D-PLSR) analysis (Eriksson et al., 2013). PLSR and D-PLSR analyses identify axes, called latent variables (LVs), which consist of profiles of cytokines or phospho-proteins that separate samples based on discrete group (i.e., sham vs. 3× CHI for D-PLSR) or continuous dependent variable (i.e., CBF or Iba1 expression for PLSR). PLSR and D-PLSR analyses were performed in MATLAB using the partial least squares algorithm by Cleiton Nunes (Mathworks File Exchange). Data were z-scored prior to inputting into the algorithm. Orthogonal rotations were applied to the sample scores and analyte weightings to obtain sample separation according to discrete group or continuous dependent variable along the LV1 axis. Error bars for LV analyte weightings were calculated by iteratively excluding samples without replacement 1000 times and regenerating the D-PLSR or PLSR model each time. Error bars in the LV plots report the mean and standard deviation (SD) computed across the PLSR or D-PLSR models generated to provide an indication of the variability within each cytokine or phospho-protein among models.

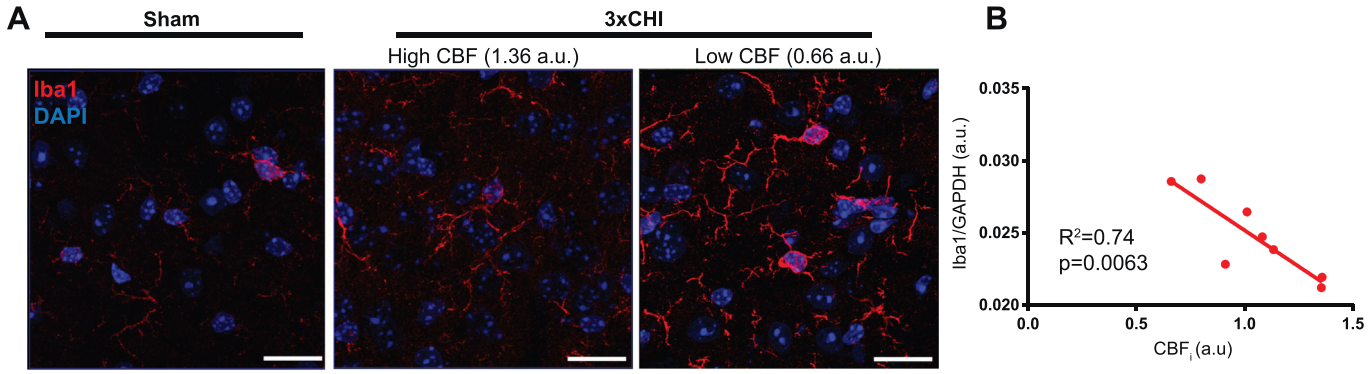

Fig. 1. Iba1 + microglial activation is inversely correlated with cerebral blood flow after 3xCHI once daily. (A) Representative cortical Iba1 immunohistochemistry of a sham mouse (left) and two 3xCHI injured mice (right) at 4 h post-impact (scale bar = 20 μm, red = Iba1, blue = DAPI). Iba1 labelling intensity modestly increases after 3xCHI. Additionally, animals with low CBF show increased Iba1 intensity and modestly enlarged microglial processes. (B) Quantitative Western blot reveals that Iba1 expression significantly inversely correlates with CBF_i measured 4 h after the third CHI (n = 8). (For interpretation of the references to colour in this figure legend, the reader is referred to the web version of this article.)

3. Results

3.1. Acute Iba1 expression is increased in mice with low cerebral blood flow after rmTBI

Mean (SEM) baseline CBF_i was 1.29 (0.10) a.u. and was not significantly different between the sham and 3xCHI groups ($p = .50$). By 4 h after 3xCHI, CBF_i in the injured group was lower than sham (1.04 (0.09) vs. 1.25 (0.18)), although this decrease was not statistically significant ($p = .10$, Table S1). Similarly, at 4 h after 3xCHI, quantitative Western blots of the microglial activation marker, Iba1, from tissue lysates isolated from the cortex showed no significant difference between injured (0.025(0.003)) and sham (0.032(0.016)) groups (normalized to GAPDH, $p = .22$).

However, inspection of Iba1 IHC images within the cortex of the injured group revealed that 3xCHI mice with low CBF 4 h after injury showed a concomitant increase in expression of Iba1, as well as moderate thickening of microglial processes (Fig. 1A). To quantitatively investigate this relationship between Iba1 expression and CBF 4 h post-injury, we used Western blot to quantify Iba1 from tissue lysates isolated from the cortex and hippocampus of 3xCHI injured animals (Fig. S1). Indeed, we observed that expression of Iba1, but not GFAP (Fig. S2), in the cortices of 3xCHI injured animals was significantly inversely correlated with CBF_i ($R = -0.86$, $p < .01$) at 4 h after 3xCHI, i.e., injured animals with the lowest cerebral blood flow were the animals with the greatest Iba1 expression (Fig. 1B). This trend was observed to a lesser extent between CBF_i and Iba1 in the cortices of sham control animals ($R = -0.75$, $p = .054$, Fig. S1B, S1D). We did not observe a significant correlation between CBF_i and Iba1 in the hippocampus of 3xCHI injured animals (Fig. S1C, S1E).

3.2. Differential expression of cytokine proteins in sham vs. injured animals after rmTBI

To further define the neuroinflammatory environment after rmTBI, we used a Luminex multiplexed immunoassay to quantify thirty-two cytokine proteins in cortical tissue lysates from both 3xCHI and sham-injured animals taken 4 h after the final injury (Fig. 2A). To account for the multidimensional nature of the data, we used a discriminant partial least square regression (D-PLSR) to identify a new variable, dubbed latent variable 1 (LV1), consisting of a weighted linear combination of cytokines that distinguishes the tissue samples of sham animals from 3xCHI animals (Fig. 2B). The weights of LV1 indicate the strength with which each individual cytokine correlates with the sham or 3xCHI groups, i.e. a greater positive weight denotes a greater degree of upregulation in 3xCHI animals whereas a greater negative weight denotes a greater degree of upregulation in sham-injured animals. Scoring each animal's sample on the LV1 axis confirms that this new variable distinguishes the sham and 3xCHI groups ($p < .001$, Fig. 2C). Further, a leave one out cross validation (LOOCV) suggests that the involvement of any one cytokine in LV1 was not due to any single sample (mean ± SD, Fig. 2B). This D-PLSR analysis identified cytokines, including IL-15, MIP-1β, M-CSF, and IL-6, that were upregulated in 3xCHI animals, along with other cytokines (e.g., VEGF, MIP-1α) that were upregulated in sham animals. Similar D-PLSR analysis in hippocampal tissue samples revealed IL-15, G-CSF, TNF-α, LIF, and MIP-1β were upregulated in 3xCHI animals, whereas IL-13 was modestly upregulated within the sham group (Fig. S3).

3.3. Cytokine protein expression correlates with low cerebral blood flow after rmTBI

Within the 3xCHI group (Fig. 3A), we used PLSR to regress the thirty-two measured cytokines against CBF_i. PLSR identified a new LV1 that distinguished 3xCHI mice by CBF_i ($p = .0003$, Fig. 3B, C). This regression revealed that mice with low CBF after 3xCHI had elevated cortical expression of chemokines (e.g., RANTES, VEGF, KC) and pro-inflammatory factors, such as IL-17, IP-10, and IL-9. Moreover, individual regression of the cytokines with the highest weights in LV1 against CBF_i showed significant individual correlations with CBF_i in the 3xCHI group but not in the sham group (Fig. 3D, Table S2). Within the sham group, PLSR against CBF_i identified different top correlates with low CBF, including IL-2, IL-9, and VEGF (Fig. S4). Plotting the cytokine weights of correlates with CBF_i for both sham and 3xCHI groups (Fig. 3E) revealed a number of cytokines that strongly correlated with low CBF_i in both groups, including VEGF, IL-2, IL-9, MIP-1α, among others. However, the strongest correlates with low CBF_i in the 3xCHI group, i.e., RANTES, IL-13, and IL-17, did not correlate in the sham group. As expected, top correlates with CBF also correlated with Iba1, including RANTES, IP-10, IL-13, VEGF, IL-17, KC, MIP-1α, and Eotaxin (Table S3). In hippocampal tissue from 3xCHI animals, TNF-α, IL-15, and IFN-γ were identified as top correlates with low CBF_i (Fig. S5).

3.4. Pro-inflammatory signaling is modulated after rmTBI

Having established that multiple markers of neuroinflammation are elevated after 3xCHI, including Iba1 and an array of pro-inflammatory cytokines, we next investigated whether or not intracellular inflammatory signaling pathways (Fig. 4A) are upregulated in 3xCHI injured animals. Luminex analysis was performed on cortical tissue lysates taken 4 h after 3xCHI or sham injury to quantify twenty-one phospho-proteins within the MAPK, phosphoinositide 3-kinase (PI3K)/

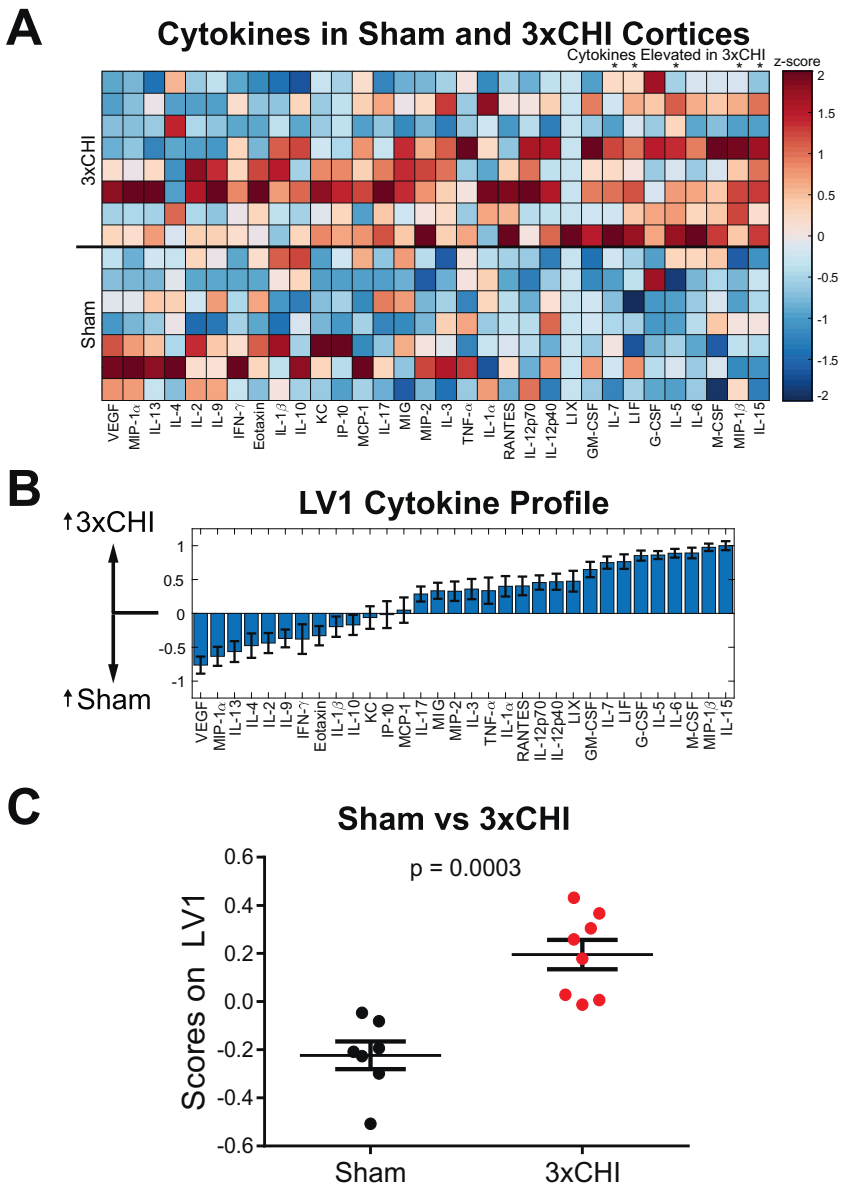

Fig. 2. Cytokine Expression Varies with CBF and Injury. (A) Multiplexed Luminex analysis of thirty-two cytokines (columns) expressed in the cortex 4 h after the third injury of 3xCHI (n = 8) and sham-injured animals (n = 7). Each row in the z-scored heat map denotes an individual animal from either the sham (bottom rows) or injured (top rows) group. Cytokines marked with an asterisk showed a significant difference ($p < .05$) between 3xCHI and sham groups. (B) Discriminant partial least squares regression identified a variable, LV1, that separated samples by experimental group. LV1 consisted of a weighted profile of cytokines that were upregulated in either 3xCHI (positive weights) or sham (negative weights) (mean ± SD across LV1 generated for all models in a leave one out cross validation). (C) Plotting each sample in terms of its cytokine score on LV1 revealed a significant difference between sham and 3xCHI groups (mean ± SEM).

Akt, and NF-κB signaling pathways (Fig. 4B). D-PLSR identified a new LV1 consisting of a weighted profile of phospho-proteins that separated 3xCHI from sham animals ($p = .0001$, Fig. 4C, D). The top phospho-proteins upregulated in 3xCHI mice spanned all three pathways and included phosphorylated Stat1, MSK1, Erk1/2, and Akt. In contrast, sham controls exhibited greater phosphorylation of IR and IRS1 than 3xCHI animals. The same analysis was conducted with hippocampal tissue lysate within the MAPK and NF-κB signaling pathways and revealed increased p-Stat1, p-Atf-2, p-MSK1, and p-Erk1/2 within the sham group but no significantly elevated signaling within the 3xCHI group (Fig. S6).

3.5. Increased MAPK and NF-κB signaling correlate with microglial activation and low cerebral blood flow after rmTBI

Within the 3xCHI group (Fig. 5A), we used PLSR to determine the extent to which these intracellular inflammatory signaling pathways correlate with the neuroinflammatory marker Iba1 (Fig. S1A). This analysis identified a weighted profile of cortical phospho-proteins from all three pathways that separated 3xCHI mice by Iba1 expression ($p < .0001$, Fig. 5B). This analysis determined that phospho-proteins within both the NF-κB and MAPK pathways most strongly correlated with Iba1 expression (p-FADD, pNF-κB, pStat1, p-p38, pJnk, pIκBα, pIKKα/β, pMSK1), whereas most proteins in the PI3K/Akt pathway did not correlate with Iba1, although phospho-Akt inversely correlated with Iba1 (Fig. 5B-C). Moreover, individual regressions of top phospho-proteins from the PLSR analysis in 3xCHI mice, including phospho-FADD, NF-κB, Stat1, p38, Jnk, and IκBα, significantly correlated with Iba1 (Fig. 5D, Table S4). Only phospho-Mek1 and Jnk significantly correlated with Iba1 among sham animals (Fig. S7). The same analysis was conducted from 3xCHI hippocampal tissue lysates for signaling within the MAPK and NF-κB signaling pathways, and revealed modest correlation of phosphorylated Jnk with Iba1, and inverse correlation of phosphorylated Mek1 and MSK1 with Iba1 (Fig. S8).

3.6. MAPK and NF-κB signaling and cytokine expression co-localized with neurons

To determine the cell type(s) responsible for elevated pro-inflammatory signaling and cytokine expression in 3xCHI injured animals, immunohistochemistry was used to co-label phospho-proteins/cytokines with the neuronal marker NeuN and the microglial marker

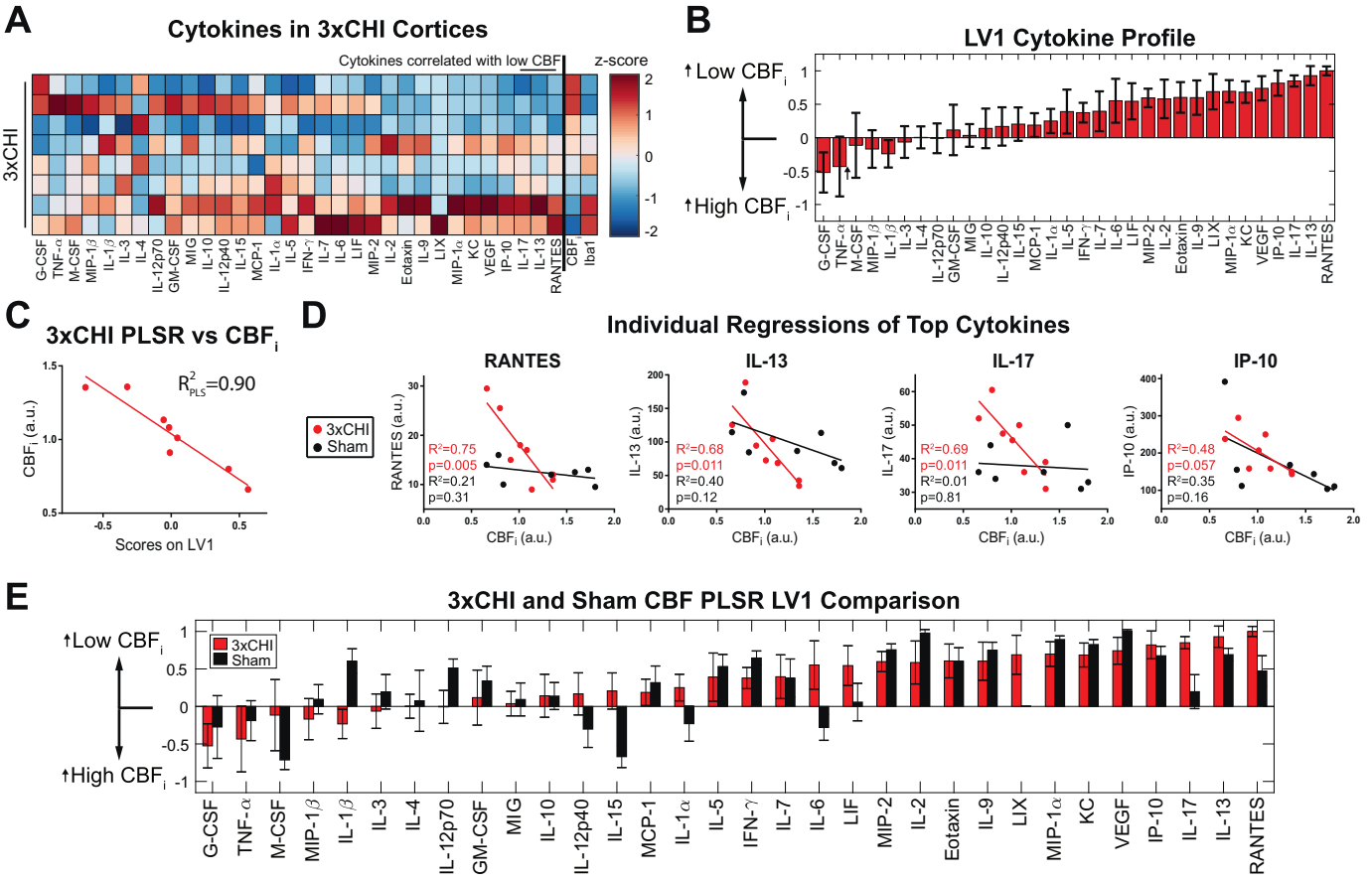

Fig. 3. Cortical cytokine expression is correlated with low CBF after 3xCHI. (A) Panel cytokine protein expression (left columns) together with CBF_i and Iba1 expression (right columns) in 3xCHI mice (n = 8, z-scored). Cytokines marked by a line overhead showed a significant linear correlation with CBF_i. (B) Partial least squares regression of 3xCHI samples against CBF_i identified a weighted profile of cytokines, LV1, that distinguished samples by CBF_i. Cytokines with negative weights were upregulated in samples with high CBF_i while cytokines with positive weights were upregulated in samples with low CBF_i (mean ± SD using a LOOCV). (C) Linear regression of LV1 scores for each sample against CBF_i. (D) Individual regressions of CBF_i against each of the cytokines with the greatest weights in LV1 for 3xCHI samples (red). These cytokines do not significantly correlate with CBF_i in the sham group (black). (E) Comparison of PLSR cytokine weights between sham black, Fig. S4) and 3xCHI groups (red) (mean ± SD using a LOOCV). (For interpretation of the references to colour in this figure legend, the reader is referred to the web version of this article.)

Iba1. Specifically, we focused on top correlates from the cytokine and phospho-protein PLSR analysis (Figs. 3 and 5), including RANTES, phospho-p38, and phospho-NF-κB. We found that both phospho-proteins and RANTES co-localized with the neuronal marker, NeuN (Fig. 6).

4. Discussion

In this study, we investigated acute neuroinflammatory changes associated with non-invasively measured CBF after repetitive mTBI. We hypothesized that low CBF in the acute phase post-injury would be associated with concomitant increases in molecular markers of inflammation. Indeed, we found that increased expression of the microglial activation marker Iba1 and pro-inflammatory cytokine profiles were correlated with low CBF after rmTBI. These data suggest that acute measurements of CBF may provide a biomarker of post-injury neuroinflammation. Indeed, since it can be non-invasively measured in humans using MRI or CT, CBF may provide a non-invasive biomarker of a pro-inflammatory tissue microenvironment post rmTBI if the findings from the present study translate to humans. Further, given our prior results demonstrating a strong correlation between low CBF and long-term cognitive deficits in mice (Buckley et al., 2015), these new data suggest a possible link between acute neuroinflammation and long-term cognitive outcomes post-rmTBI.

Among mice exposed to three once daily CHIs, we found that those with greater cortical Iba1 expression had lower CBF 4 h after 3xCHI (Fig. 1, Fig. S1A). Interestingly, this same trend, although not significant, was also observed in sham-injured animals (Fig. S1B, Fig. S1D). This commonality between sham and injured animals suggests that low CBF may be a non-invasive biomarker of underlying cortical microglial activation independent of rmTBI, although the correlation becomes more pronounced after rmTBI. Interestingly, we did not observe a relationship between CBF and hippocampal Iba1 expression, suggesting regional differences in the relationship between neuroinflammation and CBF after rmTBI (Fig. S1C, S1E). We note that Iba1 is a marker of activation of both resident microglia and macrophages, which may infiltrate the brain after TBI (Faden et al., 2016). Thus, future studies are needed to distinguish these cell types and to assess potential regional differences in the fractions of resident activated microglia vs. infiltrated peripheral immune cells after rmTBI.

Why would Iba1 correlate with cerebral blood flow? Activated microglia can produce NO, which is a potent vasodilator. However, not only do we see no difference in Iba1 between sham and injured animals, but our data reveal an *inverse* correlation between Iba1 and CBF within injured animals. If microglial release of NO alone were the link between Iba1 and CBF, we would expect to see a positive correlation between Iba1 and CBF. Notably, activated microglia post-TBI can produce superoxide that reacts with NO to form peroxynitrite, which reduces energy metabolism (Moss and Bates, 2001) and can in turn reduce blood flow. Our cytokine data provide another potential explanation for the

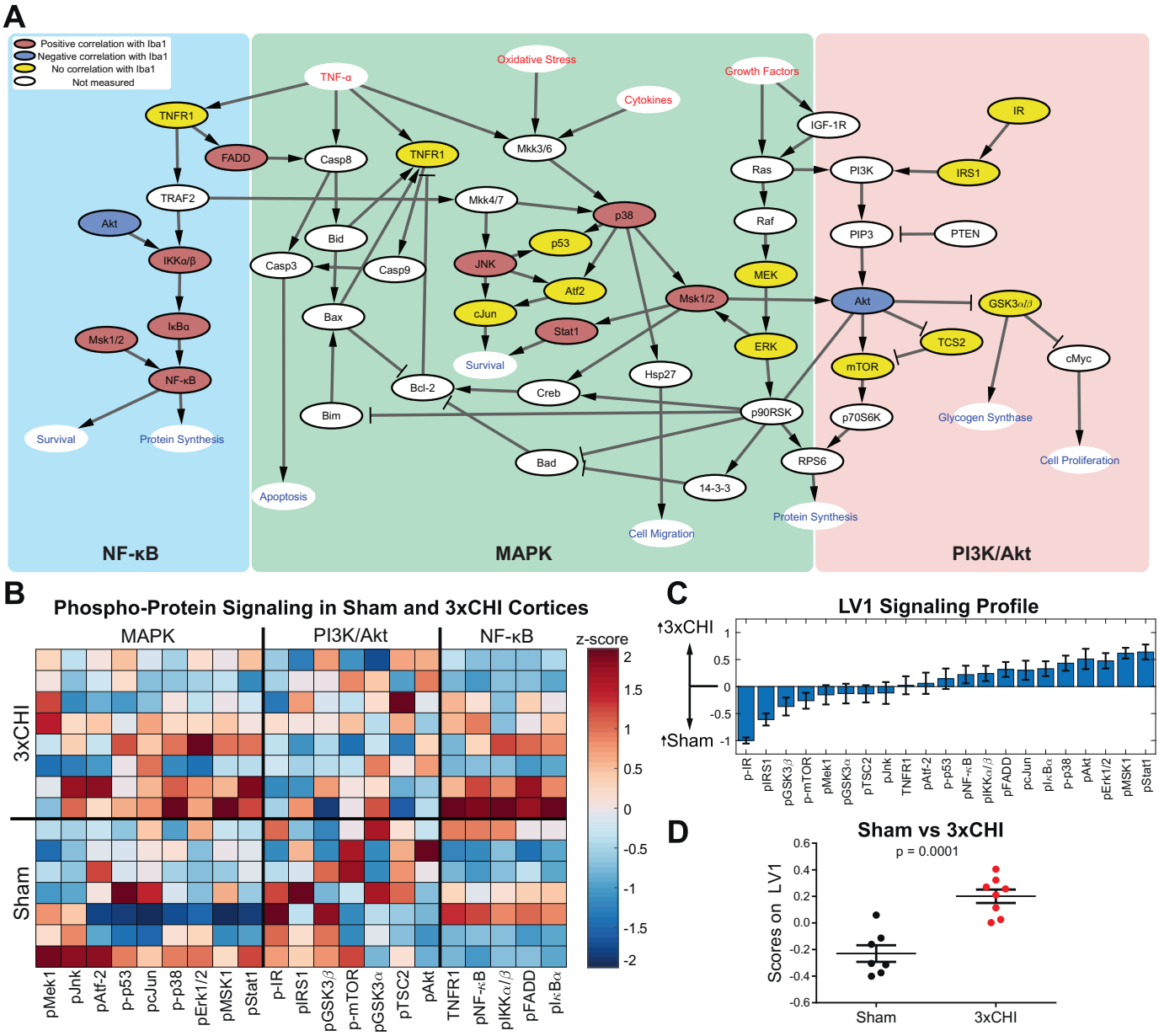

Fig. 4. Signaling is modulated within MAPK, PI3K/Akt, and NF-κB pathways after 3xCHI. (A) Intracellular signaling network diagram. Red text signifies extracellular input, blue text signifies pathway output, colored (red/blue/yellow) nodes label the twenty-one phosphoproteins measured in our analysis, while white nodes were not measured. Nodes in red denote a significant positive correlation with Iba1 in 3xCHI mice (n = 8, $p < .05$; pFADD, $p < .001$; pNFκB, $p = .001$; p-p38, $p = .001$; pIκBa, $p = .003$; pStat1, $p = .004$; pJnk, $p = .006$; pIKKα/β, $p = .007$; pMSK1, $p = .016$), nodes in blue denote a significant negative correlation with Iba1 in 3xCHI mice (n = 8; pAkt, $p = .02$). Nodes in yellow denote no significant correlation with Iba1 (Table S4). (B) Quantification of twenty-one phospho-proteins within the MAPK, PI3K/Akt, and NFκB pathways from the cortices of 3xCHI (top rows) and sham (bottom rows) mice 4 h after the third injury/sham-injured (n = 8/7; z-scored). (C) D-PLSR analysis identified a phospho-protein signaling axis, LV1, that consisted of a weighted profile of phospho-proteins that are upregulated in 3xCHI compared to sham (positive) or upregulated in sham mice compared to 3xCHI (negative) (mean ± SD using a LOOCV). (D) Plotting each sample in terms of its phospho-protein score on LV1 revealed a significant difference between sham and 3xCHI groups (mean ± SEM). (For interpretation of the references to colour in this figure legend, the reader is referred to the web version of this article.)

inverse relationship we observed between Iba1 and CBF. PLSR analysis revealed several cytokines that were upregulated in injured animals with low CBF, including RANTES, IL-13, and IL-17. RANTES is a microglial chemokine that has been implicated in microvascular dysfunction after ischemic stroke (Ances et al., 2009). IL-13 can suppress microglial NO production (Tang and Le, 2016), and IL-17 contributes to blood-brain barrier breakdown and activates glia (Waisman et al., 2015). Moreover, we found IL-15, a potent pro-inflammatory cytokine that can attenuate NO production (Hanisch et al., 1997, p. 15), to be upregulated in injured animals versus sham controls (Fig. 2). Thus, increased IL-15 expression in 3xCHI mice may simultaneously potentiate both neuroinflammation and low CBF. Taken together, these data suggest that cytokines may provide the link between Iba1 and CBF, although further studies are needed to causally prove this link.

Interestingly, a link between certain cytokines and low CBF may be present regardless of injury. We identified a number of cytokines that correlated with low CBF in *both* 3xCHI and sham groups (Fig. 3E), including IP-10 (interferon gamma-inducible protein-10), VEGF, KC (CXCL1), and MIP-1α. IP-10 promotes both microglial activation and Erk phosphorylation in neurons (Xia et al., 2000), and VEGF, MIP-1α,

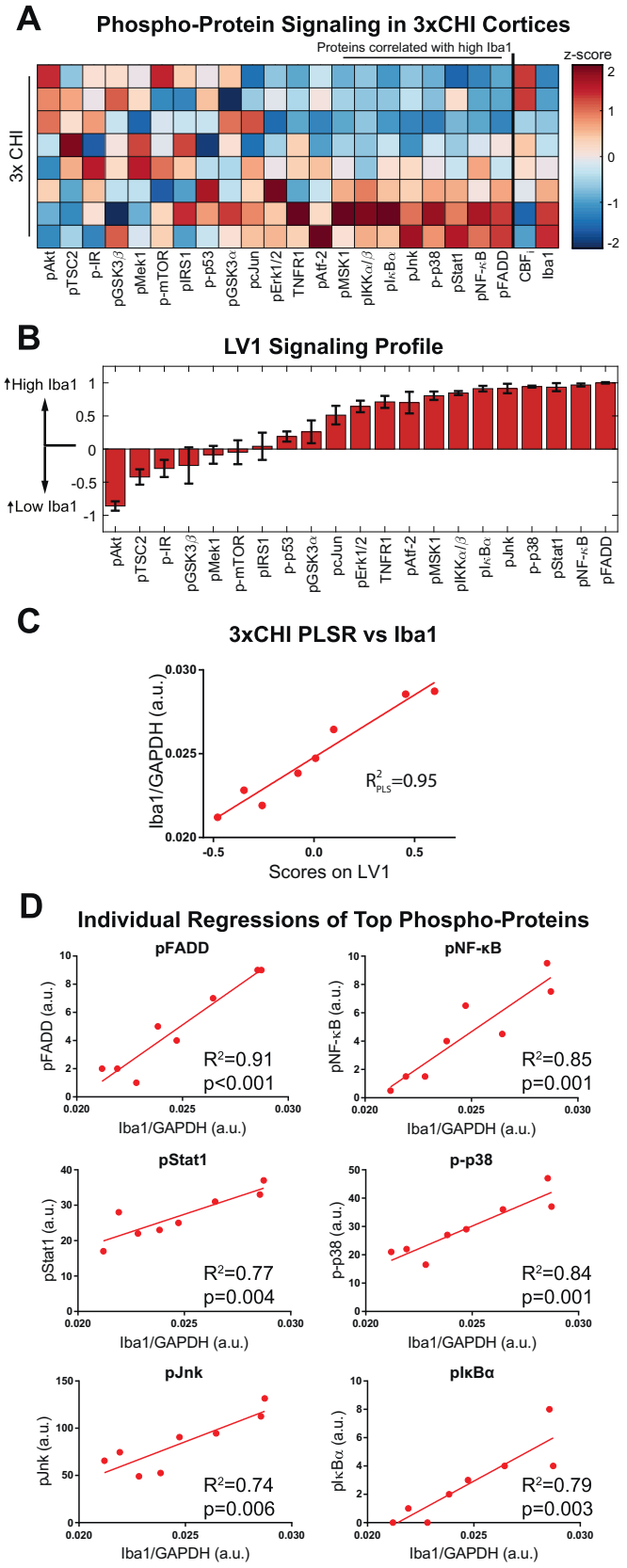

Fig. 5. Cortical phospho-protein signaling correlates with increased Iba1 after 3xCHI. (A) Panel phospho-protein signaling together with CBF_i and Iba1 expression (far right) from cortical tissue samples in 3xCHI mice. Each row denotes an individual animal (n = 8, z-scored). Phospho-proteins marked by a line overhead showed a significant positive linear correlation with Iba1. (B) Partial least squares regression of 3xCHI samples against Iba1 identified a weighted profile of phospho-proteins, LV1, that distinguished samples by Iba1. Phospho-proteins with negative weights were upregulated in samples with low Iba1 while phospho-proteins with positive weights were upregulated in samples with high Iba1 (mean ± SD using a LOOCV). (C) Linear regression of LV1 scores for each sample against Iba1. (D) Individual regressions of the phospho-proteins with the highest weights in LV1 against Iba1 for 3xCHI samples.

and KC are all microglial chemokines (Hanisch, 2002; Ryu et al., 2009). Moreover, MIP-1α and CXCL1 have been implicated in peripheral immune cell infiltration into the brain (Johnson et al., 2011). Given that we identified a correlation between Iba1 expression in both 3xCHI and sham mice, and the pro-inflammatory and chemotactic properties of the cytokines correlated with low CBF, these findings suggest that expression of neuroinflammatory mediators may be associated with low CBF, independent of injury. Given that cytokines are highly pleiotropic, it is likely that the top correlates identified in *both* sham and injury groups have both immuno- and vaso-modulatory properties. Moreover, those cytokines that only correlate with low CBF after injury (i.e., RANTES, IL-13, and IL-17) may reflect a secondary insult that may i) further modulate CBF or ii) be involved in long term cognitive deficit, which we have previously observed in mice with low CBF using this injury paradigm (Buckley et al., 2015).

Because microglial activation and cytokine expression is regulated by intracellular signaling, we hypothesized that pro-inflammatory pathways would be elevated in 3xCHI mice and would strongly correlate with markers of neuroinflammation, including Iba1. Indeed, we identified differences in phospho-protein signaling in bulk tissue between sham and 3xCHI groups (Fig. 4), and we found that within the 3xCHI group, numerous phospho-proteins within the NF-κB and MAPK pathways correlated with increased Iba1 expression (Fig. 5, Table S4). The MAPK and NF-κB pathways are both strong inflammatory regulators due to their transduction of cytokines and other extracellular signaling molecules and their downstream regulation of transcription factors that promote expression of pro-inflammatory cytokines and other inflammatory mediators (Kaminska, 2005; Rothschild et al., 2018). Thus, our results suggest that MAPK and NF-κB signaling may be responsible for acute microglial activation and cytokine expression after rmTBI.

Interestingly, MAPK and NF-κB signaling appears to be stimulated within neurons in the acute phase after 3xCHI (Figs. 5D, 6A), thus promoting neuronal expression of cytokines, specifically RANTES, (Fig. 6B) that in turn may activate microglia (Hanisch, 2002). NF-κB is a transcription factor for RANTES, which is consistent with neuronal expression (Génin et al., 2000). This neuronal response may trigger expression of cytokines such as RANTES, for which NF-κB is a transcription factor (Génin et al., 2000) (Fig. 6B). Thus, a possible explanation for our observed relationship between phospho-protein signaling and Iba1 is that stimulation of MAPK and NF-κB signaling leads to neuronal expression of cytokines that in turn activate microglia (Hanisch, 2002). Why would neurons stimulate neuroinflammation after repetitive mTBI? Signaling through both the MAPK (e.g., p38 and Jnk) and NF-κB pathways is essential to promote neuronal survival both during homeostasis and in response to stress (Farley and Watkins, 2018; Mattson and Camandola, 2001). Thus, it is possible that these pathways become activated as part of a pro-survival stress response and that expression of cytokines is a secondary consequence. Moreover, certain cytokines expressed in mice with low CBF, e.g. VEGF, have neurotrophic properties and may further stimulate neuronal survival and neurite outgrowth (Jin et al., 2002; Sanchez et al., 2010).

Finally, we note that although numerous other neuroinflammatory markers were correlated with CBF, we did not observe a relationship between CBF and the astrocyte activation marker, GFAP (Fig. S2). Astrocytes play a complex role after injury, including regulation of

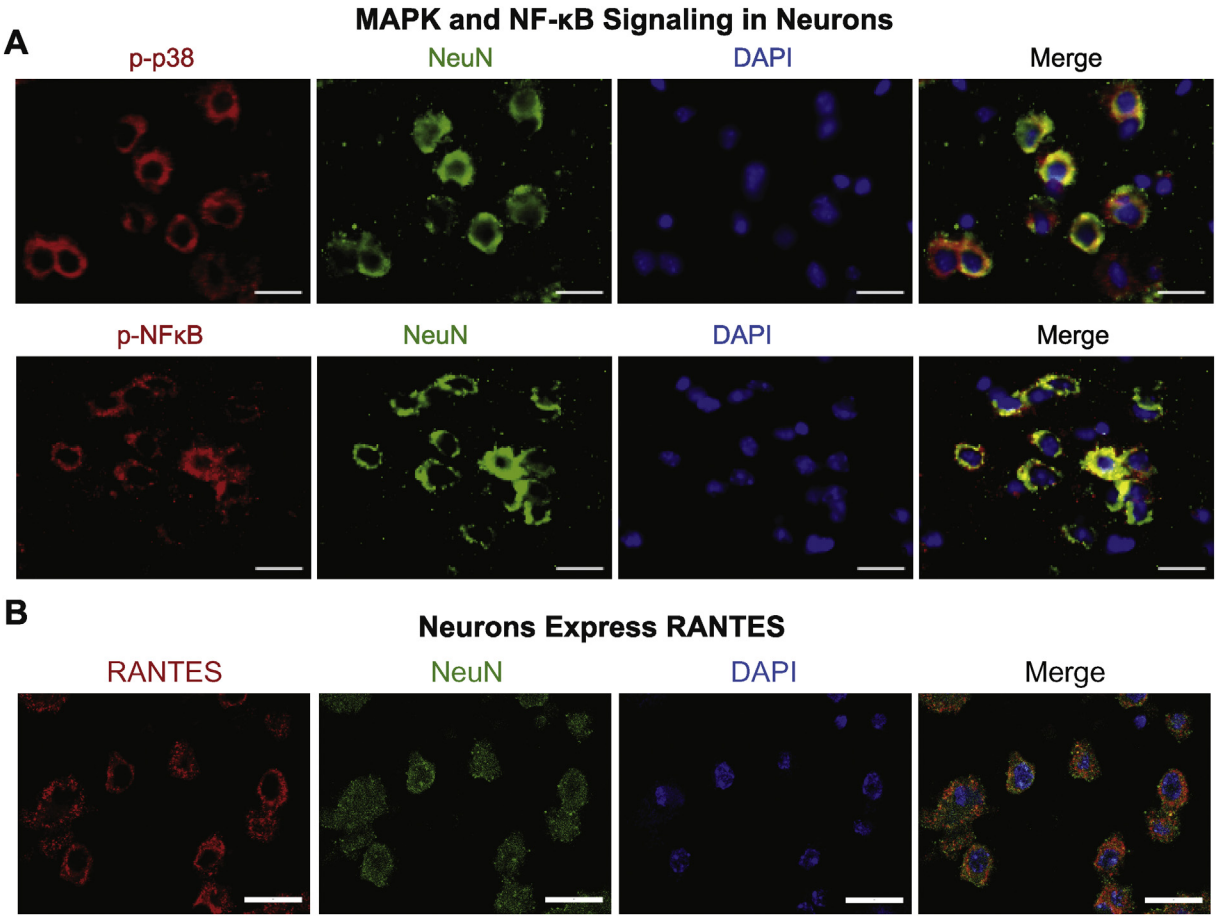

Fig. 6. MAPK, NFκB signaling and cytokine expression are localized to neurons in 3xCHI mice. (A) Representative IHC co-labeling of phospho-p38 (top panel, red) and phospho-NF-κB (bottom panel, red) with neuronal marker NeuN (green) and DAPI (blue) shows co-localization of p-p38 and p-NF-κB with neurons in a 3xCHI mouse (CBF_i = 0.66 a.u.) (scale bar = 20 μm). (B) Representative IHC co-labeling of neuronal marker NeuN (green) with RANTES (red) shows co-localization in a 3xCHI mouse (CBF_i = 0.66 a.u.) (scale bar = 20 μm). (For interpretation of the references to colour in this figure legend, the reader is referred to the web version of this article.)

vascular tone; thus, it is possible that CBF may be correlated with GFAP response, but not at the acute time point analyzed in the present study.

The present study has several limitations, suggesting several avenues of future work. First, our analysis is limited to the 4 h time point after mice have received 3xCHIs. We focused on this time point given our previous results that showed a significant correlation between cerebral blood flow at this time point and cognitive outcome at 72 h after 5xCHI (Buckley et al., 2015). Given the dynamic and evolving neuroinflammatory response, future studies of CBF, microglial and astrocyte markers, cytokine and intracellular signaling with higher temporal resolution from minutes to days after both single and multiple mTBIs are warranted to delineate the time window post-injury for which CBF may serve as a biomarker of the neuroinflammatory response. Second, the present study relies on correlation analysis to identify microglial markers, cytokines, and signaling that are associated with changes in CBF. The strength of the correlations are indicative of a causal link between them. However, future studies with small molecule inhibitors will shed insight into the causal function of both the MAPK and NF-κB pathways in regulating microglial activation, cytokine expression, and changes in CBF. Third, we used Luminex analysis so that we could rapidly collect tissues and simultaneously correlate 32 cytokines and 21 phospho-proteins against CBF and Iba-1 in an unbiased manner. Although we used IHC to begin to explore cell specificity, future studies will be needed to rigorously quantify changes in phospho-signaling and cytokine expression in a cell-type specific manner at multiple time points after each CHI. These studies may be conducted in part via IHC and fluorescent in situ hybridization approaches and will be supplemented by flow cytometric approaches to quantify phospho-signaling from isolated cell types (Simmons et al., 2015). Finally, although we have shown that CBF, and by extension long-term cognitive outcome, strongly associates with diverse markers and mediators of neuroinflammation, we have not established molecular mechanisms linking neuroinflammation and hemodynamics in the context of repetitive mTBI. Future studies targeting CBF and/or neuroinflammation will provide new insight into the relationship between CBF, neuroinflammation and long term cognitive outcome.

5. Conclusion

In total, our simultaneous collection of non-invasively measured CBF, quantified Iba1, and multiplexed analysis of cytokines and phospho-proteins from tissue homogenates isolated from the same mice gives us a unique, holistic view of the neuroinflammatory and hemodynamic events that occur after repetitive mTBI. If these results translate to humans, clinical assessment of acute CBF after mTBI may provide a surrogate marker of the degree of underlying neuroinflammatory environment. Further, the strong correlations between these parameters, together with our prior findings suggesting CBF is a surrogate for long-term cognitive deficit, implicate acute neuroinflammatory response as a potential driver of persistent cognitive deficits after repetitive mTBI. Finally, our data support future studies targeting intervention of specific inflammatory signaling pathways (i.e., MAPK and

NF-κB) as a potential therapeutic strategy for repetitive mTBI.

Declaration of conflicting interests

The author declared no potential conflicts of interest with respect to the research, authorship, and/or publication of this article.

Funding

This work was supported by the National Institutes of Health [grant number R21NS104801] and start-up funds from the Woodruff School of Mechanical Engineering at Georgia Tech and from the Coulter Department of Biomedical Engineering at Georgia Tech and Emory.

Acknowledgements

We wish to acknowledge fruitful discussions with Donald Stein, Iqbal Sayeed, and Michelle LaPlaca. We also thank the core facilities at the Parker H. Petit Institute for Bioengineering and Bioscience at the Georgia Institute of Technology for use of their shared equipment, services, and expertise. This work was funded by the National Institutes of Health award R21NS104801 (EMB), as well as start-up funds from the Woodruff School of Mechanical Engineering at Georgia Institute of Technology (LBW) and the Coulter Department of Biomedical Engineering at Georgia Institute of Technology and Emory University (EMB).

Appendix A. Supplementary data

Supplementary data to this article can be found online at https://doi.org/10.1016/j.nbd.2018.12.018.

References

Ances, B.M., Sisti, D., Vaida, F., Liang, C.L., Leontiev, O., Perthen, J.E., Buxton, R.B., Benson, D., Smith, D.M., Little, S.J., Richman, D.D., Moore, D.J., Ellis, R.J., HNRC group, 2009. Resting cerebral blood flow: a potential biomarker of the effects of HIV in the brain. Neurology 73, 702–708. https://doi.org/10.1212/WNL.0b013e3181b59a97.

Armstead, W.M., 2006. Differential activation of ERK, p38, and JNK MAPK by nociceptin/orphanin FQ in the potentiation of prostaglandin cerebrovasoconstriction after brain injury. Eur. J. Pharmacol. 529, 129–135. https://doi.org/10.1016/j.ejphar.2005.08.059.

Barkhoudarian, G., Hovda, D.A., Giza, C.C., 2016. The molecular pathophysiology of concussive brain injury - an update. Phys. Med. Rehabil. Clin. N. Am. 27, 373–393. https://doi.org/10.1016/j.pmr.2016.01.003.

Buckley, E.M., Miller, B.F., Golinski, J.M., Sadeghian, H., McAllister, L.M., Vangel, M., Ayata, C., Meehan III, W.P., Franceschini, M.A., Whalen, M.J., 2015. Decreased microvascular cerebral blood flow assessed by diffuse correlation spectroscopy after repetitive concussions in mice. J. Cereb. Blood Flow Metab. 35, 1995–2000. https://doi.org/10.1038/jcbfm.2015.161.

Chao, C.C., Hu, S., Molitor, T.W., Shaskan, E.G., Peterson, P.K., 1992. Activated microglia mediate neuronal cell injury via a nitric oxide mechanism. J. Immunol. (Baltim. Md.) 1950 (149), 2736–2741.

da Costa, L., van Niftrik, C.B., Crane, D., Fierstra, J., Bethune, A., 2016. Temporal profile of cerebrovascular reactivity impairment, gray matter volumes, and persistent symptoms after mild traumatic head injury. Front. Neurol. 7, 70. https://doi.org/10.3389/fneur.2016.00070.

Durduran, T., Yodh, A.G., 2014. Diffuse correlation spectroscopy for non-invasive, microvascular cerebral blood flow measurement. NeuroImage 85 (Pt 1), 51–63. https://doi.org/10.1016/j.neuroimage.2013.06.017.

Eriksson, L., Byrne, T., Johansson, E., Trygg, J., Vikström, C., 2013. Multi- and Megavariate Data Analysis Basic Principles and Applications. Umetrics Academy.

Faden, A.I., Wu, J., Stoica, B.A., Loane, D.J., 2016. Progressive inflammation-mediated neurodegeneration after traumatic brain or spinal cord injury. Br. J. Pharmacol. 173, 681–691. https://doi.org/10.1111/bph.13179.

Farley, M.M., Watkins, T.A., 2018. Intrinsic neuronal stress response pathways in injury and disease. Annu. Rev. Pathol. Mech. Dis. 13, 93–116. https://doi.org/10.1146/annurev-pathol-012414-040354.

Forbes, J.A., Awad, A.J., Zuckerman, S., Carr, K., Cheng, J.S., 2012. Association between biomechanical parameters and concussion in helmeted collisions in American football: a review of the literature. Neurosurg. Focus. 33, E10. https://doi.org/10.3171/2012.9.FOCUS12288.

Génin, P., Algarté, M., Roof, P., Lin, R., Hiscott, J., 2000. Regulation of RANTES chemokine gene expression requires cooperativity between NF-kappa B and IFN-regulatory factor transcription factors. J. Immunol. (Baltim. Md.) 1950 (164), 5352–5361.

Giza, C.C., Hovda, D.A., 2014. The new neurometabolic cascade of concussion. Neurosurgery 75 (Suppl. 4), S24–S33. https://doi.org/10.1227/NEU.0000000000000505.

Goodwin, J.L., Uemura, E., Cunnick, J.E., 1995. Microglial release of nitric oxide by the synergistic action of beta-amyloid and IFN-gamma. Brain Res. 692, 207–214.

Guskiewicz, K.M., McCrea, M., Marshall, S.W., Cantu, R.C., Randolph, C., Barr, W., Onate, J.A., Kelly, J.P., 2003. Cumulative effects associated with recurrent concussion in collegiate football players: the NCAA concussion study. JAMA 290, 2549–2555. https://doi.org/10.1001/jama.290.19.2549.

Hanisch, U.K., 2002. Microglia as a source and target of cytokines. Glia 40, 140–155. https://doi.org/10.1002/glia.10161.

Hanisch, U.K., Neuhaus, J., Quirion, R., Kettenmann, H., 1996. Neurotoxicity induced by interleukin-2: involvement of infiltrating immune cells. Synapse 24, 104–114. https://doi.org/10.1002/(SICI)1098-2396(199610)24:2<104::AID-SYN2>3.0.CO;2-J.

Hanisch, U.K., Lyons, S.A., Prinz, M., Nolte, C., Weber, J.R., Kettenmann, H., Kirchhoff, F., 1997. Mouse brain microglia express interleukin-15 and its multimeric receptor complex functionally coupled to Janus kinase activity. J. Biol. Chem. 272, 28853–28860. https://doi.org/10.1074/jbc.272.46.28853.

Ikeda-Matsuo, Y., Ikegaya, Y., Matsuki, N., Uematsu, S., Akira, S., Sasaki, Y., 2005. Microglia-specific expression of microsomal prostaglandin E2 synthase-1 contributes to lipopolysaccharide-induced prostaglandin E2 production. J. Neurochem. 94, 1546–1558. https://doi.org/10.1111/j.1471-4159.2005.03302.x.

IOM, NRC, 2014. Sports-Related Concussions in Youth: Improving the Science, Changing the Culture. The National Academies Press, Washington, D.C.

Jin, K., Zhu, Y., Sun, Y., Mao, X.O., Xie, L., Greenberg, D.A., 2002. Vascular endothelial growth factor (VEGF) stimulates neurogenesis in vitro and in vivo. Proc. Natl. Acad. Sci. U. S. A. 99, 11946–11950. https://doi.org/10.1073/pnas.182296499.

Johnson, E.A., Dao, T.L., Guignet, M.A., Geddes, C.E., Koemeter-Cox, A.I., Kan, R.K., 2011. Increased expression of the chemokines CXCL1 and MIP-1α by resident brain cells precedes neutrophil infiltration in the brain following prolonged soman-induced status epilepticus in rats. J. Neuroinflammation 8, 41. https://doi.org/10.1186/1742-2094-8-41.

Kaminska, B., 2005. MAPK signalling pathways as molecular targets for anti-inflammatory therapy–from molecular mechanisms to therapeutic benefits. Biochim. Biophys. Acta 1754, 253–262. https://doi.org/10.1016/j.bbapap.2005.08.017.

Liu, W., Wang, B., Wolfowitz, R., Yeh, P.H., Nathan, D.E., Graner, J., Tang, H., Pan, H., Harper, J., Pham, D., Oakes, T.R., French, L.M., Riedy, G., 2013. Perfusion deficits in patients with mild traumatic brain injury characterized by dynamic susceptibility contrast MRI. NMR Biomed. 26, 651–663. https://doi.org/10.1002/nbm.2910.

Longhi, L., Saatman, K.E., Fujimoto, S., Raghupathi, R., Meaney, D.F., Davis, J., McMillan, B.S.A., Conte, V., Laurer, H.L., Stein, S., Stocchetti, N., McIntosh, T.K., 2005. Temporal window of vulnerability to repetitive experimental concussive brain injury. Neurosurgery 56, 364–374.

Mattson, M.P., Camandola, S., 2001. NF-κB in neuronal plasticity and neurodegenerative disorders. J. Clin. Invest. 107, 247–254.

Meehan 3rd, W.P., Zhang, J., Mannix, R., Whalen, M.J., 2012. Increasing recovery time between injuries improves cognitive outcome after repetitive mild concussive brain injuries in mice. Neurosurgery 71, 885–891. https://doi.org/10.1227/NEU.0b013e318265a439.

Meier, T.B., Bellgowan, P.S.F., Singh, R., Kuplicki, R., Polanski, D.W., Mayer, A.R., 2015. Recovery of cerebral blood flow following sports-related concussion. JAMA Neurol. 72, 530–538. https://doi.org/10.1001/jamaneurol.2014.4778.

Mez, J., Daneshvar, D.H., Kiernan, P.T., et al., 2017. Clinicopathological evaluation of chronic traumatic encephalopathy in players of american football. JAMA 318, 360–370. https://doi.org/10.1001/jama.2017.8334.

Moss, D.W., Bates, T.E., 2001. Activation of murine microglial cell lines by lipopolysaccharide and interferon-gamma causes NO-mediated decreases in mitochondrial and cellular function. Eur. J. Neurosci. 13, 529–538.

Patterson, M.S., Andersson-Engels, S., Wilson, B.C., Osei, E.K., 1995. Absorption spectroscopy in tissue-simulating materials: a theoretical and experimental study of photon paths. Appl. Opt. 34, 22–30. https://doi.org/10.1364/ao.34.000022.

Rothschild, D.E., McDaniel, D.K., Ringel-Scaia, V.M., Allen, I.C., 2018. Modulating inflammation through the negative regulation of NF-κB signaling. J. Leukoc. Biol. https://doi.org/10.1002/JLB.3MIR0817-346RRR.

Ryu, J.K., Cho, T., Choi, H.B., Wang, Y.T., McLarnon, J.G., 2009. Microglial VEGF receptor response is an integral chemotactic component in Alzheimer's disease pathology. J. Neurosci. 29, 3–13. https://doi.org/10.1523/JNEUROSCI.2888-08.2009.

Sanchez, A., Wadhwani, S., Grammas, P., 2010. Multiple neurotrophic effects of VEGF on cultured neurons. Neuropeptides 44, 323–331. https://doi.org/10.1016/j.npep.2010.04.002.

Simmons, A.J., Banerjee, A., McKinley, E.T., Scurrah, C.R., Herring, C.A., Gewin, L.S., Masuzaki, R., Karp, S.J., Franklin, J.L., Gerdes, M.J., Irish, J.M., Coffey, R.J., Lau, K.S., 2015. Cytometry-based single-cell analysis of intact epithelial signaling reveals MAPK activation divergent from TNF-α-induced apoptosis in vivo. Mol. Syst. Biol. 11, 835. https://doi.org/10.15252/msb.20156282.

Talavage, T.M., Nauman, E.A., Breedlove, E.L., Yoruk, U., Dye, A.E., Morigaki, K.E., Feuer, H., Leverenz, L.J., 2014. Functionally-detected cognitive impairment in high school football players without clinically-diagnosed concussion. J. Neurotrauma 31, 327–338. https://doi.org/10.1089/neu.2010.1512.

Tang, Y., Le, W., 2016. Differential Roles of M1 and M2 Microglia in Neurodegenerative Diseases. Mol. Neurobiol. 53, 1181–1194. https://doi.org/10.1007/s12035-014-9070-5.

Waisman, A., Hauptmann, J., Regen, T., 2015. The role of IL-17 in CNS diseases. Acta

Neuropathol. (Berl.) 129, 625–637. https://doi.org/10.1007/s00401-015-1402-7.
Wu, L., Chung, J.Y., Saith, S., Tozzi, L., Buckley, E.M., Sanders, B., Franceschini, M.A., Lule, S., Izzy, S., Lok, J., Edmiston, W.J., McAllister, L.M., Mebane, S., Jin, G., Lu, J., Sherwood, J.S., Willwerth, S., Hickman, S., Khoury, J.E., Lo, E.H., Kaplan, D., Whalen, M.J., 2018. Repetitive head injury in adolescent mice: a role for vascular inflammation. J. Cereb. Blood Flow Metab. Off. J. Int. Soc. Cereb. Blood Flow Metab. https://doi.org/10.1177/0271678X18786633. (271678X18786633).
Xia, M.Q., Bacskai, B.J., Knowles, R.B., Qin, S.X., Hyman, B.T., 2000. Expression of the chemokine receptor CXCR3 on neurons and the elevated expression of its ligand IP-10 in reactive astrocytes: in vitro ERK1/2 activation and role in Alzheimer's disease. J. Neuroimmunol. 108, 227–235.